
Article:
Warneke, C., Trainer, M., de Gouw, J. A. et al. (48 more authors) (2016) Instrumentation and Measurement Strategy for the NOAA SENEX Aircraft Campaign as Part of the Southeast Atmosphere Study 2013. Atmospheric Measurement Techniques. pp. 3063-3093. ISSN 1867-8548

https://doi.org/10.5194/amt-2015-388

Atmos. Meas. Tech. Discuss., doi:10.5194/amt-2015-388, 2016
Manuscript under review for journal Atmos. Meas. Tech.
Published: 20 January 2016

Atmospheric Measurement Techniques Discussions

Instrumentation and Measurement Strategy for the NOAA SENEX Aircraft Campaign as Part of the Southeast Atmosphere Study 2013

Warneke C.[1,2], M. Trainer[2], J.A. de Gouw[1,2], D.D. Parrish[1,2], D.W. Fahey[2], A.R. Ravishankara[2,9], A.M. Middlebrook[2], C.A. Brock[2], J.M. Roberts[2], S.S. Brown[2], J.A. Neuman[1,2], B.M. Lerner[1,2], D. Lack[1,2], D. Law[1,2], G. Hübler[1,2], I. Pollack[1,2,9], S. Sjostedt[1,2], T.B. Ryerson[2], J.B. Gilman[1,2], J. Liao[1,2], J. Holloway[1,2], J. Peischl[1,2], J.B. Nowak[1,2,10], K. Aikin[1,2], K.-E. Min[1,2,11], R.A. Washenfelder[1,2], M.G. Graus[1,2,12], M. Richardson[1,2], M.Z. Markovic[1,2,13], N.L. Wagner[1,2], A. Welti[1,2,14, 14], P.R. Veres[1,2], P. Edwards[1,2, 15], J.P. Schwarz[2], T. Gordon[1,2], W.P. Dube[1,2], S. McKeen[1,2], J. Brioude[1,2], R. Ahmadov[1,2], A. Bougiatioti[3], J. Lin[3], A. Nenes[3], G.M. Wolfe[4,16], T.F. Hanisco[4], B.H. Lee[5], F.D. Lopez-Hilfiker[5], J.A. Thornton[5,19], F.N. Keutsch[6,17], J. Kaiser[6], J. Mao[7,18], C. Hatch[8]

[1] Cooperative Institute for Research in Environmental Sciences, Univ. of Colorado, Boulder
[2] Chemical Sciences Division, NOAA Earth System Research Laboratory, Boulder, CO
[3] Georgia Institute of Technology, Atlanta, GA
[4] NASA Goddard Space Flight Center, Greenbelt, MD
[5] University of Washington
[6] University of Wisconsin-Madison, Madison, WI
[7] Geophysical Fluid Dynamics Laboratory, NOAA, Princeton, NJ
[8] Department of Chemistry, Hendrix College, 1600 Washington Ave., Conway, AR, USA
[9] now at Department of Atmospheric Science, Colorado State University, Ft Collins, CO, USA
[10] now at Aerodyne Research Inc., Billerica, MA
[11] now Gwangju Institute of Science and Technology, Gwangju, Korea
[12] now at Institute of Atmospheric and Cryospheric Sciences University of Innsbruck, Austria
[13] now at Air Quality Processes Research Section, Environment Canada, Toronto, Ontario, Canada
[14] now at Leibniz Institute for Tropospheric Research
[15] now at University of York, UK
[16] University of Maryland Baltimore County
[17] now at Harvard University, Cambridge, MA
[18] Princeton University
[19] now at Laboratory of Atmospheric Chemistry, Paul Scherrer Institute, Villigen, Switzerland

Atmos. Meas. Tech. Discuss., doi:10.5194/amt-2015-388, 2016
Manuscript under review for journal Atmos. Meas. Tech.
Published: 20 January 2016

Atmospheric Measurement Techniques Discussions

Abstract:

The Southeast United States (US) might not have warmed as much as the rest of the country over the past 50-100 years. Providing an improved understanding of this potential anomaly, and specifically the roles played by aerosols, was one of the main goals for the Southeast Atmosphere Study (SAS). Natural emissions of ozone-and-aerosol-precursor gases such as isoprene and monoterpenes are high in the southeast of the US. In addition, anthropogenic emissions are significant in the Southeast US and summertime photochemistry is rapid. The NOAA-led SENEX (Southeast Nexus) aircraft campaign was one of the major components of the SAS study and was focused on studying the interactions between biogenic and anthropogenic emissions to form secondary pollutants. During SENEX, the NOAA WP-3D aircraft conducted 20 research flights between 27 May and 10 July 2013 based out of Smyrna, TN.

Here we describe the experimental approach, the science goals and early results of the NOAA SENEX campaign. The aircraft, its capabilities and standard measurements are described. The instrument payload is summarized including detection limits, accuracy, precision and time resolutions for all gas-and-aerosol phase instruments. The inter-comparisons of compounds measured with multiple instruments on the NOAA WP-3D are presented and were almost all within the stated uncertainties.

The SENEX flights included day- and nighttime flights in the Southeast as well as flights over areas with intense shale gas extraction (Marcellus, Fayetteville and Haynesville shale). We present one example flight on 16 June 2013, which was a daytime flight over the Atlanta region, where several crosswind transects of plumes from the city and nearby point sources, such as power plants, paper mills and landfills, were flown. The area around Atlanta has large biogenic isoprene emissions, which provided an excellent case for studying the interactions between biogenic and anthropogenic emissions. In this example flight, chemistry in and outside the Atlanta plumes was observed for several hours after emission. The analysis of this flight showcases the strategies implemented to answer some of the main SENEX science questions.

Atmos. Meas. Tech. Discuss., doi:10.5194/amt-2015-388, 2016
Manuscript under review for journal Atmos. Meas. Tech.
Published: 20 January 2016

Atmospheric Measurement Techniques Discussions

1. Introduction

The SENEX campaign (Southeast Nexus-Studying the Interactions between Natural and Anthropogenic Emissions at the Nexus of Climate Change and Air Quality) was a large-scale National Oceanic and Atmospheric Administration (NOAA) led field study in the Southeastern United States (U.S.) in summer 2013. The SENEX measurement platform was the NOAA WP-3D aircraft operated out of Smyrna, Tennessee. SENEX was part of a large, comprehensive and coordinated research effort to understand the emission sources, chemistry, and meteorology of the summertime atmosphere in the Southeast U.S.: the Southeast Atmosphere Study (SAS) (Xu et al., 2015), which included the other field campaigns: Southern Oxidant and Aerosol Study (SOAS), Tropospheric HONO (TropHONO), and the North American Airborne Mercury Experiment (NAAMEX). Besides the NOAA WP-3D, measurements during SAS were made on the following platforms and locations: the National Science Foundation (NSF) National Center for Atmospheric Research (NCAR) C-130 aircraft, the Purdue University Duchess aircraft, the State University of New York-Stony Brook Long-EZ aircraft, the Centreville and Alabama Aquatic Biodiversity Centre (AABC) flux ground site located in Alabama, the Look Rock, Tennessee ground site, the Research Triangle Park (RTP) ground site in North Carolina and Caltech chamber studies (FIXIT).

The detailed science goals for SENEX can be found in the SENEX white paper (http://esrl.noaa.gov/csd/projects/senex/) and are briefly listed here:

(1) Understanding the emissions of aerosol, aerosol and ozone (O_3) precursors, and greenhouse gases in the Southeast U.S. Special focus was aimed at evaluating available emission inventories for organic aerosol, black carbon, NO_x ($NO+NO_2$), volatile organic compounds (VOCs), sulfur dioxide (SO_2), greenhouse gases, and aerosol precursors from point sources such as coal-fired power plants, urban areas as well as biogenic VOC emissions. Another focus was to understand the importance of emissions from biomass burning in the region.

(2) Understanding the formation mechanisms of secondary species such as ozone, sulfate and organic aerosols in the Southeast U.S. The main focus here was to determine the influence of biogenic emissions, nighttime chemistry, aqueous-phase processes, and organic nitrates on the formation of the secondary species.

Atmos. Meas. Tech. Discuss., doi:10.5194/amt-2015-388, 2016
Manuscript under review for journal Atmos. Meas. Tech.
Published: 20 January 2016

Atmospheric Measurement Techniques Discussions

(3) Determining the composition and distribution of aerosol in the Southeast U.S. by looking at the relative abundance of sulfate, organics and other chemical components over the whole study region and at accessible altitude levels.

(4) Quantifying deposition and loss processes critical for determining atmospheric concentrations of aerosol, ozone and NO_y (sum of nitrogen oxides).

(5) Determining the climate-relevant properties of aerosol in the Southeast U.S. by looking at the extinction, absorption and CCN properties of aerosol from primary and secondary sources and their dependence on the high humidity in the Southeast U.S. Special focus was given on determining the fraction of organic aerosol that occurs naturally versus the fraction that is controlled by anthropogenic emissions and how each may change in the future as a result of warming and changes in anthropogenic emissions. Additional focus was on black carbon and its co-emitted species to understand whether controlling specific BC sources has a net warming or cooling effect.

(6) Quantifying methane (CH_4) and VOC emissions from selected shale gas extraction regions (Marcellus, Haynesville and Fayetteville).

In this paper we describe the payload of the NOAA WP-3D, describe the locations of the SENEX flights, show inter-comparisons used to evaluate the measurements and describe an example flight to showcase the measurement strategies that were used during SENEX.

2. NOAA WP-3D aircraft

The two NOAA WP-3D aircraft have been used in air quality and climate related airborne field campaigns since 1994. The NOAA WP-3D carried its maximum payload of 3600 kg of scientific equipment during SENEX and 4-6 scientists. The aircraft has a range of 3000 km and a ceiling of about 7600 m. During SENEX the highest altitude was about 6400 m due to the heavy payload. Flight duration was typically around 7 hr, and the majority of the flights were conducted in the daytime boundary layer approx. 0.5 km above ground level. A picture of the aircraft taken during SENEX is shown in Figure 1.

The WP-3D was equipped by the NOAA Aircraft Operations Center (AOC) flight facility with instruments detailing the position and motion of the aircraft as well as many meteorological parameters such as 3D wind speed and direction, ambient, potential and

Atmos. Meas. Tech. Discuss., doi:10.5194/amt-2015-388, 2016
Manuscript under review for journal Atmos. Meas. Tech.
Published: 20 January 2016

Atmospheric Measurement Techniques Discussions

dew point temperatures, water vapor mixing ratios, pressure and sea surface temperature. A list of the most commonly used aircraft-provided parameters and their uncertainties is given in Table 1.

3. NOAA WP-3D SENEX flight summaries

During SENEX a total of 20 research flights were conducted; of those, two were test flights from Tampa, Florida and two were the transfer flights between Tampa, FL and Smyrna, TN. All of the flights, including the test and transfer flights, addressed multiple science goals. All the SENEX flight tracks are shown in Figure 2 on a map of the Southeast US that also shows most of the larger point sources in the region. Twelve daytime, three nighttime and five shale gas region flights (Marcellus, Haynesville and Fayetteville shale) were conducted to answer the major SENEX science questions. The flight tracks in Figure 2 are color-coded by those three categories and details about each flight can be found in Tables 2, 3, and 4, where a short description of the flight, the investigated emission sources, and the coordinating activities are listed.

4. NOAA WP-3D SENEX chemical and aerosol instrumentation

The WP-3D instrumentation payload on the WP-3D was specifically designed to provide the necessary measurements to answer the SENEX science questions. The instrumentation included a wide variety of gas and aerosol-phase measurements. A schematic drawing of the payload of the WP-3D is shown in Figure 1b. All the instruments for aerosol phase measurements are listed in Table 5 and for gas phase measurements in Table 6 together with their measurement technique, accuracy and precision, sample interval, and a reference to a publication describing the respective instrument in detail. Overall 22 different instruments were installed on the NOAA WP-3D with a total power consumption of 40 A (110V, 400 Hz 3 phase), 130 A (110V, 400 Hz), 40A (110V 60 Hz), and 42 A (28 V DC). Most instruments were mounted inside the fuselage, but two instrumented wingpods added significant scientific payload capacity including 72 whole-air canister samples, a carbon monoxide (CO) analyzer and the fine particle counter to add significant scientific payload capacity. Four to six scientists were on board during each flight to monitor all the instruments and adjust the flight plans to current meteorological

Atmos. Meas. Tech. Discuss., doi:10.5194/amt-2015-388, 2016
Manuscript under review for journal Atmos. Meas. Tech.
Published: 20 January 2016

Atmospheric Measurement Techniques Discussions

conditions as needed. During the flights, selected aircraft and instrument data were streamed to the ground and could be monitored in near real time on a website for situational awareness for all SONGNEX scientists.

A detailed description for each instrument can be found in the SI; in the following two paragraphs the instrument name and measurement technique are given and in Tables 5 and 6, accuracy, precision, sample interval and literature reference are listed in addition.

Aerosol-phase measured parameters were: (1) the particle (0.004-8.3μm) number, size and volume with parallel condensation particle counters (CPCs) and white and laser light scattering, (2) sub-micrometer extinction and absorption of dry, humidified, and thermodenuded aerosol at three wavelengths spanning the visible with a cavity ringdown aerosol extinction spectrometer (CRD) and a photoacoustic aerosol absorption spectrometer (PAS), (3) the non-refractory submicron aerosol composition of organics, sulfate, nitrate, ammonium and chloride with an aerosol mass spectrometer (AMS), (4) cloud condensation nuclei (CCN) and supersaturation, (5) accumulation-mode refractory black carbon (rBC) mass content of single particles with an SP2. Most of the aerosol instrumentation was connected to a low turbulence inlet (LTI) (Wilson et al., 2004), which slows down the sample flow from aircraft speeds to 5 m/s generating minimal turbulence and improving particle transmission.

Gas-phase measurements were: (1) the greenhouse gases carbon dioxide (CO_2) and methane (CH_4) with wavelength scanned cavity ringdown spectroscopy, (2) two measurements of nitric oxide (NO) and O_3, each measured by gas-phase chemiluminescence (CL) and by cavity ringdown absorption spectroscopy (CRDS), three measurements of nitrogen dioxide (NO_2), by UV photolysis and gas-phase chemiluminescence (P-CL) and by CRDS and by airborne cavity enhanced absorption spectroscopy (ACES), NO_y by gold-catalyzed thermal conversion and gas-phase CL, (3) carbon monoxide (CO) with vacuum UV resonance fluorescence, (4) SO_2 with pulsed UV fluorescence, (5) ammonia (NH_3), nitric acid (HNO_3), and two measurements of nitrous acid (HONO), and formic acid (HCOOH) with chemical ionization mass spectrometry (CIMS), and (6) the nighttime oxidants NO_3 and N_2O_5 with CRDS and CIMS. Various volatile organic compounds (VOCs) were measured with several different techniques: (7)

Atmos. Meas. Tech. Discuss., doi:10.5194/amt-2015-388, 2016
Manuscript under review for journal Atmos. Meas. Tech.
Published: 20 January 2016

Atmospheric Measurement Techniques Discussions

oxygenates, aromatics, isoprene, monoterpenes and acetonitrile with Proton-Transfer-Reaction Mass Spectrometry (PTR-MS); (8) hydrocarbons, halocarbons and a few selected oxygenates from canister samples and post-flight GC-MS analysis (iWAS/GCMS); (9) formaldehyde with the In Situ Airborne Formaldehyde (ISAF) using laser induced fluorescence (LIF); (10) glyoxal with ACES; (11) organic and inorganic acids by UW-TOF-CIMS; and (12) peroxyacyl nitrates PANs and nitryl chloride ($ClNO_2$) with a separate CIMS. In addition up and down welling photolysis rates (j_{NO2} and j_{O3}) were measure with filter radiometers.

5. Inter-comparison of Duplicate Measurements on the WP-3D

Some parameters were measured by more than one instrument on the WP-3D, giving opportunities for inter-comparisons and the results are described in the following.

Three instruments measured NO_2: P-CL, CRDS, and ACES. The agreement between CRDS and ACES with the standard P-CL technique, as shown in Figure 3, was on average 6% and 10% and the measurements were correlated with a linear correlation coefficient (R^2) of 0.99 and 0.93, respectively. The agreement is within the combined uncertainties, given in Table 6, for CRDS and just outside for ACES and P-CL. Two instruments measured ozone: P-CL and CRDS and the inter-comparison is also shown in Figure 3. The ozone measurements correlated with R^2 of 0.96 and agreed on average within 8%, which is within the combined measurement uncertainties of the two instruments as given in Table 6. All the data for the whole campaign were included for this inter-comparison using 1-second ozone data; NO_2 data were averaged to the 5-second ACES time resolution. Two instruments measured NO: CL and CRDS, with the CRDS data subject to an optical instability that degraded the detection limit during this campaign. The large majority of the data were below this degraded detection limit, and therefore the inter-comparison was not included here.

Several VOCs were measured on the WP-3D with both the PTR-MS and with iWAS/GCMS. As an example the isoprene time series for the flight on June 29, 2013 is shown for both instruments in Figure 4. For the purpose of this comparison, the PTR-MS data are averaged over an interval that starts 10 s before and stops 10 s after the canister filling time to ensure at least one PTR-MS data point was used in the comparison. Isoprene

Atmos. Meas. Tech. Discuss., doi:10.5194/amt-2015-388, 2016
Manuscript under review for journal Atmos. Meas. Tech.
Published: 20 January 2016

Atmospheric Measurement Techniques Discussions

has a very high variability in the boundary layer, due to its short lifetime and high emissions. This variability and imperfect time alignment causes a large part of the scatter observed in Figure 4. The scatter plots for the inter-comparison of isoprene and other VOCs are shown in Figure 4 as well. The comparison had slopes between 0.64-1.45, which is just within the combined uncertainties of the two instruments given in Table 6, and R^2 of 0.5 or higher. The iWAS/GCMS was deployed during SENEX for the first time and some instrument issues occurred, causing some degradation of the data quality compared to previous inter-comparisons (de Gouw and Warneke, 2007; Warneke et al., 2011). More details on the instrument performance during SENEX, the inter-comparison and the stability of VOCs, especially oxygenates, in canisters can be found in Lerner at al (2015).

Two instruments measured formic acid (HCOOH): the HNO_3-CIMS and the University of Washington high-resolution time-of-flight chemical ionization mass spectrometer (UW HR-ToF-CIMS) and their comparison is shown in Figure 5. The time series shows results from one individual flight and the scatter plot shows all data from the campaign, where the color code indicates the individual flights. The comparison using all the data has a slope of 1.03 and R^2 of 0.80, while the slopes of individual flights ranged from 1.40 to 0.66 with R^2 always higher than 0.91. The reason for the flight-to-flight variability in their agreement is yet unknown. The output of the continuously added ^{13}C formic acid permeation device – to which the UW HR-ToF-CIMS instrument sensitivity was referenced (see SI) – may have contributed to the variability of the reported formic acid mixing ratio between flights, because an independent method of quantification of its output was not available (Veres et al., 2010). Cross calibrations were not conducted between the two instruments during the campaign and therefore do not allow direct comparisons of instrument sensitivity on a flight-to-flight basis. Nevertheless, the variability between the two measurements is within the combined uncertainties of the two instruments (±20% for HNO_3-CIMS and ±50% for UW HR-ToF-CIMS).

During the night flights two instruments measured $ClNO_2$: the UW HR-ToF-CIMS and the PAN-CIMS and N_2O_5 was measured with the UW HR-ToF-CIMS and CRDS. The comparison is shown in Figure 6 as time series and scatter plots for the flight on 07/03/2013. The slopes are 1.19 and 0.91 and the R^2 0.74 and 0.92, respectively. For small signals such as $ClNO_2$, the signal to noise of the UW HR-ToF-CIMS is aided by its

Atmos. Meas. Tech. Discuss., doi:10.5194/amt-2015-388, 2016
Manuscript under review for journal Atmos. Meas. Tech.
Published: 20 January 2016

Atmospheric Measurement Techniques Discussions

ability to distinguish isobaric contaminants from halogen containing molecules, which have a distinct mass defect (Kercher et al., 2009; Lee et al., 2014). The scatter plot displays some non-linearity and the N_2O_5 is just outside the range of a previous comparison (Chang et al., 2011), but the results are within the combined uncertainties of the instruments given in Table 6.

Figure 7 shows the NO_y budget for all the individually measured NO_y species compared to the measured total NO_y for the NOAA WP-3D flight on June 16, 2013. Aerosol nitrate might contribute about 2% to the sum. This assumes a quantitative sampling and conversion of aerosol nitrate. This is likely not the case and NO_y from aerosol nitrate is likely an upper limit and the data are shown with and without the potential aerosol contribution. The highest mixing ratios of NO_y are observed in power plant plumes, where most NO_y consists of NO_x. For a more detailed comparison the NO_z (=NO_y-NO_x) budget is shown in Figure 7 as well. The power plant plumes were removed for this comparison, because the time resolution and the accuracy of NO_y and NO_x are not high enough to calculate small differences in NO_z during these periods with very high NO_x mixing ratios. On this flight the sum of individually measured NOy constituents was roughly 90% of the total measured as NOy, similar to the whole campaign NO_y budget. The unmeasured NO_y outside power plants was about 25% (or 15%, when including aerosol nitrate). This missing fraction may be comprised largely of organic nitrates derived from the oxidation of isoprene and monoterpene (Lee et al., 2014).

The aerosol volume derived from the chemical composition data (AMS and SP2) was compared to the volume derived from the measured size distributions, following Middlebrook et al. (2012). All of these measurements sampled aerosol downstream of a 1 micron impactor. For each 10-s AMS measurement, the composition-derived volume was calculated by adding the average rBC mass from the SP2 instrument to the AMS total aerosol mass and dividing it by the density estimated from the AMS and BC composition. The mass-weighted density (ρ) was calculated using ρ_{org} = 1.25 g cm^{-3} (Cross et al., 2007; Kiendler-Scharr et al., 2009; Zelenyuk et al., 2008), ρ_{inorg} = 1.75 g cm^{-3} (primarily dry ammonium sulfate, (Perry and Green, 1997)), and ρ_{BC} = 1.8 g cm^{-3} (Park et al., 2004), for organic mass, inorganic mass, and BC, respectively. The measured AMS lens transmission curve (Bahreini et al., 2008) was applied to the particle number distributions to account

Atmos. Meas. Tech. Discuss., doi:10.5194/amt-2015-388, 2016
Manuscript under review for journal Atmos. Meas. Tech.
Published: 20 January 2016

for particle transmission losses in the AMS lens before calculating the volume from the size distributions, which were also averaged over the AMS sampling time. For this field project, the fraction of aerosol volume behind the 1 micron impactor that was transmitted into the AMS instrument by the lens was on average 99% with a minimum of 92%.

The composition-derived volume was then plotted against the volume calculated from the size distributions for each flight with available data. Resulting slopes are depicted in Figure 8 as a function of flight date color coded with the linear correlation coefficient R^2. The grey bands indicate the overall combined 2σ uncertainty of ±60% (Bahreini et al., 2009; Brock et al., 2011; Schwarz et al., 2006). The volumes from most of the flights agree within this combined uncertainty and with R^2 values between 0.62 to 0.98, indicating that most of the aerosol in the AMS lens transmission size-range was composed of non-refractory material and black carbon. Only the slopes for flights on 29 June 2013 was outside the uncertainty band. We note that rBC only contributed 1% on average to the total accumulation mode mass, and in 1-min averages only exceeded 3% less than 1% of the time during SENEX.

On June 29, 2013 the NOAA WP-3D and the NSF NCAR C-130 did coordinated wing-to-wing flight legs in the free troposphere and the boundary layer for an inter-comparison in southern Tennessee and northern Alabama with a duration of just over one hour. Several over-flights over the SOAS ground site in Centreville were performed during SENEX. Results of the platform inter-comparisons will not be presented here.

6. Example Flight on 16 June 2013 near Atlanta, GA

Results from the SENEX research flight on 16 June 2013 are presented here to demonstrate the strategy used to address many of the SENEX science questions such as the determination of anthropogenic and biogenic emissions, and the subsequent atmospheric chemistry, transformation, and production of secondary species. Flights over the shale gas regions will not be discussed here, but calculations of the methane emission fluxes from the three shale gas regions can be found elsewhere (Peischl et al., 2015; Yuan et al., 2015). The major goal of the 16 June 2013 flight was to investigate the Atlanta urban plume and the Scherer and Harllee Branch power plant plumes as they were transported over heavily forested areas in Georgia with strong biogenic emissions.

Atmos. Meas. Tech. Discuss., doi:10.5194/amt-2015-388, 2016
Manuscript under review for journal Atmos. Meas. Tech.
Published: 20 January 2016

Atmospheric Measurement Techniques Discussions

315

316 6.1 Anthropogenic, biogenic and point source emissions

317 Figure 9a shows the WP-3D flight track over Atlanta and surrounding areas color-
318 coded by NO_y on top of a map showing anthropogenic emission sources, which are the
319 urban areas and point sources: power plants, landfills, paper mills and coal mines. Other
320 point sources studied that are not shown on this map include bio-fuel refineries (de Gouw
321 et al., 2015a). The point sources are sized by their respective emission strengths or
322 capacity. The flight included eight tracks perpendicular to the wind direction (numbered
323 0-7 in Figure 9a): one upwind of Atlanta, three over the metro area and four downwind.
324 The flight tracks were set such that the distance between each leg represents about 1 hour
325 of transport at the prevailing wind speed and also such that many of the point source
326 plumes were intercepted.

327 Figure 10 shows results for the intercepts of such point source plumes. In Figure
328 10a the methane measurements along transect 4 downwind of the Pine Bluff landfill in
329 Georgia are shown. Landfills are an important source of methane in the US, but they do not
330 emit many other compounds and indeed methane was the only species measured aboard
331 the WP-3D payload that showed a detectable enhancement in the plume. The forested
332 Southeast US is heavily managed for large-scale wood and wood products and therefore
333 has a large density of pulp and paper mills. Pulp and paper mills use a significant amount
334 of energy, which they often produce partially on site. For example the investigated facility
335 has four steam producing boilers at close to 80 MWh that mainly burn coal, natural gas, oil
336 and wood/bark waste biomass. The power production results in emissions of the
337 combustion species NO, NO_2, CO, SO_2 and CO_2 (only NO is shown in Figure 10b). The paper
338 mill plumes were intercepted on transect 0 during this flight. High mixing ratios of
339 monoterpenes, methanol and acetaldehyde were also observed downwind of those
340 facilities (Figure 10b).

341 U.S. urban emissions, and therefore urban mixing ratios of many air pollutants have
342 decreased significantly over the last few decades (Dallmann and Harley, 2010; Emmons et
343 al., 2015; von Schneidemesser et al., 2010; Warneke et al., 2012). For example, Warneke et
344 al. (2012) analyzed 50 years of ambient measurements and found that VOCs and CO have
345 decreased at an annual rate of about 7.5% in Los Angeles, CA. Blanchard et al. (2015)

Atmos. Meas. Tech. Discuss., doi:10.5194/amt-2015-388, 2016
Manuscript under review for journal Atmos. Meas. Tech.
Published: 20 January 2016

Atmospheric Measurement Techniques Discussions

346 analyzed Southeastern Aerosol Research and Characterization (SEARCH) network data
347 and found downward trends in ambient carbon monoxide (CO), sulfur dioxide (SO_2), and
348 oxidized nitrogen species (NO_y) concentrations averaged 1.2 ± 0.4 to 9.7 ± 1.8% per year
349 from 1999 to 2010. The NOAA WP-3D flew over Atlanta, GA during SOS (Southern Oxidant
350 Study 1999) on 6 July 1999 and the results are shown in Figure 11 and are compared to
351 the SENEX 16 June 2013 data. These two days were comparable in meteorological
352 conditions with wind speeds around 4 m/s, temperatures around 26 degrees C in the
353 boundary layer, and boundary layer heights of about 1.6 km on 6 July 1999 and 1-1.2 km
354 on 16 June 2013. The flight track on top of the map color coded with 1999 NO_y shows
355 qualitatively that the pollution was more intense and widespread. The time series of CO
356 and NO_y for the two flights in Figure 11 are consistent with significant emissions decreases
357 between 1999 and 2013. It is expected that the comparison between the 1999 and 2013
358 airborne data sets will provide important insights and evidence to answer the main
359 science questions from SENEX.
360
361 6.2 Coal and natural gas fired power plant plumes
362 During SENEX several power plant plumes were sampled. Figure 12 shows the
363 flight track from the 22 June 2013 over Atlanta that included transects downwind of the
364 coal fired Bowen and the natural gas combined cycle McDonough power plants. The
365 emission intensities of these two different kinds of power plants are very different;
366 combined cycle natural gas power plant have much lower CO_2, SO_2 and NO_x emissions per
367 unit energy produced than coal fired power plants (de Gouw et al., 2014). The Bowen
368 power plant produced 3.3 TWh and McDonough 4.7 TWh in the 1st quarter of 2013.
369 According to the continuous emissions monitoring systems (CEMS) monitoring data,
370 during the 1st quarter of 2013 the Bowen power plant emitted 930 g/kWh CO_2, 0.20
371 g/kWh SO_2 and 0.56 g/kWh NO_x, while McDonough emitted 360 g/kWh CO_2, 0.0019
372 g/kWh SO_2 and 0.018 g/kWh NO_x. These large differences in emission intensities are
373 clearly reflected in the enhancements measured in the downwind transects shown in
374 Figure 12. In the Bowen power plant plume about 20 ppmv CO_2, 5 ppbv NO_y and 4 ppbv
375 SO_2 enhancements were observed, while the McDonough plume had only about 5 ppmv of
376 CO_2 enhancement and SO_2 and NO_y were not measurably enhanced above background. To

Atmos. Meas. Tech. Discuss., doi:10.5194/amt-2015-388, 2016
Manuscript under review for journal Atmos. Meas. Tech.
Published: 20 January 2016

account for the different dilutions during transport (5km distance for Bowen and 10 km for McDonough at about 3m/s average wind speed) enhancement ratios need to be considered. In the Bowen plume 0.24 ppb/ppm of NO_y/CO_2 and 0.13 ppb/ppm of SO_2/CO_2 were measured. Because no enhancements in the McDonough plume were seen, enhancement ratios cannot be determined, but using a S/N=2 the upper limit for enhancement ratios in the McDonough plume are 0.06 ppb/ppm for of NO_y/CO_2 and 0.11 ppb/ppm for SO_2/CO_2 are determined. This shows that the NO_y and SO_2 enhancements in the gas fired McDonough plant are clearly smaller than in the coal fired Bowen plant. In addition to investigating emissions from the power plant plumes as was shown here, the emissions of those power plants mix with the large emissions of isoprene in this area as can be seen in Figure 9. This provides an ideal case for studying the interactions between natural and anthropogenic emissions. The chemistry of isoprene, OH, formaldehyde and NO_x in power plant plumes and other areas during SENEX will be described in detail elsewhere (de Gouw et al., 2015b; Kaiser et al., 2015; Wolfe et al., 2015).

6.3 Modeling Support for SENEX

Figure 13 shows example results from one of the modeling tools that is available for analysis of the SENEX results, the Lagrangian particle dispersion model FLEXPART (Stohl et al., 2005). From locations along the flight tracks, 20,000 particles were released in the model and tracked for 10 days backward in time. The model outputs the residence time of the particles in a volume such as the surface layer. By multiplying the footprint with gridded emission fluxes the model calculates the mixing ratio of the emitted species at the location of the aircraft. All species are considered as conserved tracers; the model does not contain chemical transformations, but it does keep track of the time since emission. As an example, Figure 13 a and b show the time series of FLEXPART NO_y (accumulating emissions from the previous 48 hours) together with the flight track color coded with NO_y. Comparing the modeled and measured NO_y in Figure 13a and Figure 9, it can be seen that the model reproduces the time series qualitatively, including the broader features and the power plant plume encounters. The very high mixing ratios in the narrow power plant plumes are underestimated in the model (the plumes are too narrow for the model resolution). The footprint map for a point along the last flight track downwind of

Atmos. Meas. Tech. Discuss., doi:10.5194/amt-2015-388, 2016
Manuscript under review for journal Atmos. Meas. Tech.
Published: 20 January 2016

Atmospheric Measurement Techniques Discussions

the Harllee Branch power plant plume is shown in Figure 13c showing that the mixing ratios at this point along the flight track will have the highest contribution from the immediate upwind area that includes the Harllee Branch power plant, just as expected. But there was also a significant contribution to the mixing ratios from long-range transport from the Northeast US. Other available FLEXPART model outputs include CO, biomass burning CO, SO_2, isoprene and monoterpenes. Besides FLEXPART other models are (or will be) also available including the NOAA AM3 model (http://esrl.noaa.gov/csd/projects/senex/), an MCM-based 0-D box model (Wolfe et al., 2015) and WRF-Chem (Weather Research and Forecasting with Chemistry) simulations.

7. Summary

The Southeast Atmosphere Study (SAS) was a large collaborative and community effort to understand the air quality and climate issues in the Southeast United States. This paper provides a summary of the experimental setup for the NOAA-led SENEX study, which was an important component of the SAS. The NOAA WP-3D aircraft capabilities, the payload, instrument descriptions, inter-comparisons and flight locations and goals are described in detail in this paper. The flight on 16 June 2013 in the Atlanta area was described in some detail to demonstrate the strategies used during SENEX to study the air quality and climate relevant interactions of biogenic and anthropogenic emissions in the Southeast, which was one of the main foci of the SAS study.

ACKNOWLEDGMENT

The US Weather Research Program within NOAA/OAR Office of Weather and Air Quality supported S. McKeen and R. Ahmadov. We are grateful M. Dumas (NOAA Holling's Scholar), D. Hughes, and A. Jaksich from Hendrix College for their help with the iWAS2 measurements. Participation of ISAF was enabled by US EPA Science to Achieve Results (STAR) program grant 83540601.

Atmos. Meas. Tech. Discuss., doi:10.5194/amt-2015-388, 2016
Manuscript under review for journal Atmos. Meas. Tech.
Published: 20 January 2016

Atmospheric Measurement Techniques Discussions

436 **Tables**
437
438 **Table 1:** Standard NOAA WP-3D provided parameters
439

Aircraft Parameters	Technique	Units	Uncertainty
aircraft position	GPS latitude	deg	±16m
	GPS longitude	deg	±16m
	GPS altitude	m	±16m
	pressure altitude	m	±10m
	radar altitude above ground	m	±15m or 1-2%
aircraft meteorology	ambient temperature	deg C	±0.5C
	dew point temperature	deg C	±0.5C
	TDL dew point temperature	deg C	5%
	H_2O mixing ratio*	g/kg	5%
	potential temperature	deg K	±0.5K
	relative humidity*	%	±5%
	static pressure	mb	±2.2mb
	vertical wind speed	m/s	±0.5m/s
	wind direction	deg	5 deg
	wind speed	m/s	1 m/s
aircraft miscellaneous	attack angle	deg	±0.2 deg
	cabin pressure	mb	N/A
	ground speed	m/s	±3.4m/s
	heading	deg	±0.5 deg
	pitch angle	deg	±0.05 deg
	roll angle	deg	±0.05 deg
	slip angle	deg	±0.2 deg
	true air speed	m/s	±0.5 m/s

440 * H_2O mixing ratio and relative humidity are derived from dew point temperature
441

Atmos. Meas. Tech. Discuss., doi:10.5194/amt-2015-388, 2016
Manuscript under review for journal Atmos. Meas. Tech.
Published: 20 January 2016

Atmospheric Measurement Techniques Discussions

442 **Table 2:** Fight descriptions for the NOAA WP-3D daytime flights in the SE US
443

Flight Date in 2013	Day of the week	Description	Investigated Emission Source
5/29	Wednesday	Testflight in Florida Jacksonville St John's River	biogenic urban power plant
5/31	Friday	Testflight in Florida Jacksonville St John's River	biogenic urban power plant
6/03	Monday	Transfer Tampa to Smyrna Birmingham EC Gaston, Johnsonville, Cumberland, Colbert Centreville spiral	 urban power plant coal mine
6/11	Tuesday	Centreville Birmingham west to east EC Gaston	 urban power plant
6/12	Wednesday	Atlanta west to east Scherer, Bowen, Yates, Wansley, Harlee Branch	urban power plant
6/16	Sunday	Atlanta southwest to northeast on weekend Scherer, Bowen, Yates, Wansley, Harlee Branch paper mills, landfills poultry farming	urban power plant point sources agriculture
6/18	Tuesday	Aborted flight, circled over Franklin	
6/22	Saturday	Birmingham and Atlanta west to east Centreville EC Gaston coal mines, land fills, paper mills	urban power plant point sources
6/23	Sunday	Indianapolis biogenic/landscape emission change Johnsonville, Cumberland	urban biogenic power plant
6/29	Saturday	Centreville C-130 inter-comparison Birmingham James H Miller Jr, EC Gaston	 urban power plant
7/05	Friday	Ozarks St Louis Archer Daniels Midland biofuel refinery	biogenic urban point source
7/10	Wednesday	Transfer flight Smyrna to Tampa coal mines, paper mill hog farming	 point sources agriculture

444
445
446

Atmos. Meas. Tech. Discuss., doi:10.5194/amt-2015-388, 2016
Manuscript under review for journal Atmos. Meas. Tech.
Published: 20 January 2016

Atmospheric Measurement Techniques Discussions

447 **Table 3:** Fight descriptions for the NOAA WP-3D nighttime flights in the SE US
448

Flight Date in 2013	Day of the week	Description	Investigated Emission Sources
6/19	Wednesday	Atlanta day into night Missed approaches step profile in aged Atlanta plume	urban
7/02	Tuesday	Birmingham north to south Centreville JH Miller, EC Gaston, Gorgas, US Steel, Greene County	urban power plants
7/03	Wednesday	New Madrid, White Bluff agricultural fire	power plants biomass burning

449
450
451 **Table 4:** Fight descriptions for the NOAA WP-3D flights in shale gas regions
452

Flight Date in 2013	Day of the week	Shale Play	Additional Investigated Emission Sources
6/10	Monday	Haynesville	
6/25	Tuesday	Haynesville	
6/26	Wednesday	Fayetteville	Biogenics in Ozarks Independence power plant
7/06	Saturday	Marcellus	
7/08	Monday	Fayetteville	New Madrid power plant

453
454
455

Atmos. Meas. Tech. Discuss., doi:10.5194/amt-2015-388, 2016
Manuscript under review for journal Atmos. Meas. Tech.
Published: 20 January 2016

Atmospheric Measurement Techniques Discussions

456 **Table 5:** Aerosol instrumentation on the NOAA WP-3D during SENEX
457

Measurement	Name/Technique	Accuracy	Precision	Sample Interval	Reference
Low turbulence inlet	LTI: decelerating inlet to provide sample air to aerosol instruments in fuselage	N/A	N/A	N/A	(Wilson et al., 2004)
Size distributions fine (0.004-1μm) and coarse (1-8.3μm)	parallel CPCs, and white and laser light scattering			1s	(Brock et al., 2011; Brock et al., 2000)
Cloud condensation nuclei (CCN) and supersaturation	CCN: Continuous-flow streamwise thermal-gradient CCN counter with scanning flow CCN analysis	10% 0.04% super-saturation	10 CCN cm^{-3}	30-60s	(Lance et al., 2006; Roberts and Nenes, 2005)
8 cell optical extinction (dry 405, 532, 662nm, 70% and 90% RH 532nm, thermodenuded 405 and 662nm)	CRD: Cavity ringdown aerosol extinction spectrometer	<2%	10% 0.1 Mm^{-1}	1s	(Langridge et al., 2011)
5 cell optical absorption (dry 405, 532, 662nm, thermodenuded 405nm and 662nm)	PAS: Photoacoustic Absorption Spectrometer	10 %	1 Mm^{-1}	1s	(Lack et al., 2012)
Refractory BC mass content of individual particles	SP2: Single-Particle Soot Photometer with laser-induced incandescence	30%	0.5 fg (0.08 μm mass-equiv. diameter with 2 g/cc density)	1s	(Schwarz et al., 2008; Schwarz et al., 2010)
Non-refractory, submicron sulfate, nitrate, ammonium, organic and chloride mass concentrations	AMS: Aerosol Mass Spectrometer	50%	0.05, 0.07, 0.24, 0.36, and 0.05 μg sm^{-3} (study average)	10s	(Bahreini et al., 2009)
Cloud particle size distribution (0.6-50μm) (3-50μm) (50-6000μm)	Cloud probes: Laser light forward and back scattering Laser light forward scattering Droplet imaging probe			1s	(Lance et al., 2010)

458
459

Atmos. Meas. Tech. Discuss., doi:10.5194/amt-2015-388, 2016
Manuscript under review for journal Atmos. Meas. Tech.
Published: 20 January 2016

Atmospheric Measurement Techniques Discussions

460 **Table 6:** Gas-phase instrumentation on the NOAA WP-3D during SENEX
461

Measurement	Technique	Accuracy	Precision or Detec. Limit	Sample Interval	Reference
CH_4 CO_2	wavelength-scanned cavity ring-down absorption spectroscopy	0.07 ppm 1 ppb	0.11 ppm 0.4 ppb	1s	(Peischl et al., 2012)
CO	vacuum UV resonance fluorescence	5%	0.5ppb	1s	(Holloway et al., 2000)
SO_2	pulsed UV fluorescence	20%	250ppt	1s	(Ryerson et al., 1998)
NO NO_2 NO_y O_3	Gas phase chemiluminescence	3% 4% 12% 2%	10ppt 30ppt 40ppt 15ppt	1s	(Pollack et al., 2010; Ryerson et al., 1998; Ryerson et al., 1999)
various VOCs	PTR-MS: proton transfer reaction mass spectrometer using H_3O^+ as reagent ion	25%	depending on signal and species	1s every 17s	(de Gouw and Warneke, 2007)
hydrocarbons, oxygenated VOCs	iWAS: whole air sampler with immediate GC-MS analysis	12-20% % %	4-7ppt ppt ppt	72/flight (3-8s)	(Gilman et al., 2009; Lerner et al., 2015)
HNO_3 HCOOH HONO	HNO_3-CIMS: chemical ionization mass spectrometer with I^- as reagent ion	20%+50ppt 20%+120ppt 40%+30 ppt	25 ppt 40 ppt 25 ppt	1s	(Neuman et al., 2002; Neuman et al., 2003)
NH_3	NH_3-CIMS: chemical ionization mass spectrometer with protonated acetone dimers as reagent ion	25%+(0.02-0.5) ppb (depending on flight)	0.02-0.07 ppb (depending on flight)	1s	(Neuman et al., 2003; Nowak et al., 2007)
PAN PPN APAN $ClNO_2$	PAN-CIMS: chemical ionization mass spectrometry with I- as reagent ion	0.04-0.05ppb 0.04-0.1ppb 0.01-0.02ppb 0.01-0.02ppb	0.01ppb 0.003ppb 0.006ppb 0.02ppb	2s	(Osthoff et al., 2008; Slusher et al., 2004; Zheng et al., 2011)
various oxygenated VOCs $ClNO_2$ N_2O_5 alkyl nitrates	UW HR-ToF-CIMS: chemical ionization mass spectrometer with I^- as reagent ion	50%	depending on signal and species	1s	(Lee et al., 2014)
glyoxal NO_2	ACES: cavity enhanced absorption spectroscopy	5.8% 5%	34 pptv 80 ppt	10s 5s	(Min et al., 2015; Washenfelder et al., 2011)
NO NO_2 O_3 NO_3 N_2O_5	CRDS: cavity ring-down absorption spectrometer	5% 5% 10% 20% 12%	1 ppbv 0.2 ppbv 0.2 ppbv 3 pptv 3 pptv	1s	(Dube et al., 2006; Wagner et al., 2011)
HCHO	In Situ Airborne Formaldehyde (ISAF): laser induced fluorescence	10%	36ppt	1s	(Cazorla et al., 2015; DiGangi et al., 2011; Hottle et al., 2009)
j_{NO2} and j_{O1D}	j-heads: filter radiometers	10%		1s	

462
463

Atmos. Meas. Tech. Discuss., doi:10.5194/amt-2015-388, 2016
Manuscript under review for journal Atmos. Meas. Tech.
Published: 20 January 2016

Atmospheric Measurement Techniques Discussions

464 **Figures:**
465
466

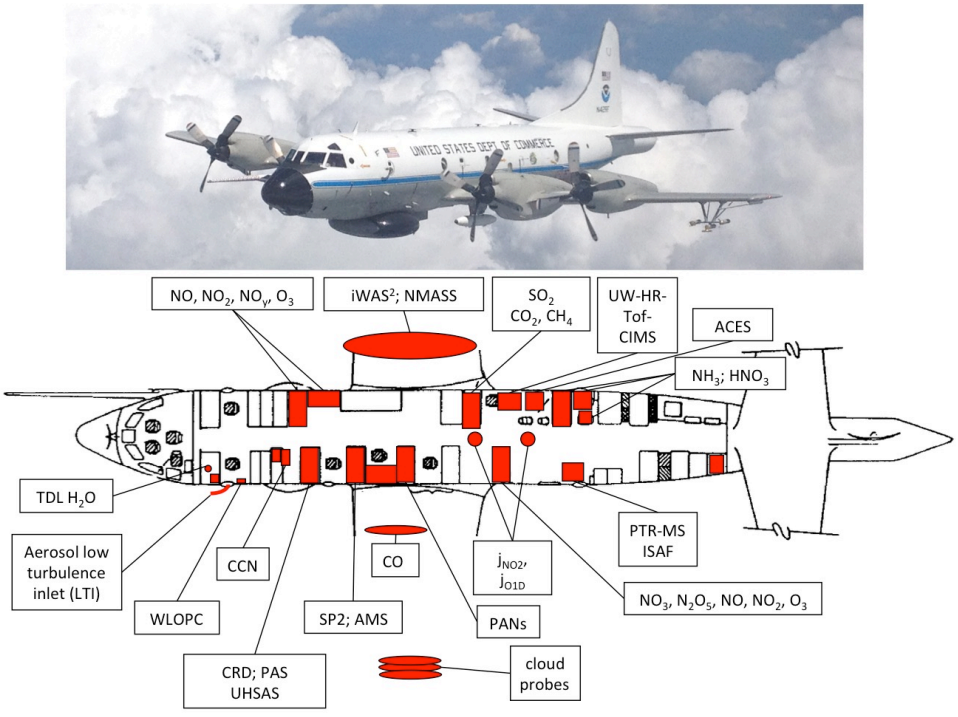

467
468
469 **Figure 1:** NOAA WP-3D aircraft picture, payload and layout. The photo was taken during
470 the inter-comparison flight with the NCAR C-130 by Lynne Gratz.
471
472

Atmos. Meas. Tech. Discuss., doi:10.5194/amt-2015-388, 2016
Manuscript under review for journal Atmos. Meas. Tech.
Published: 20 January 2016

Atmospheric Measurement Techniques Discussions

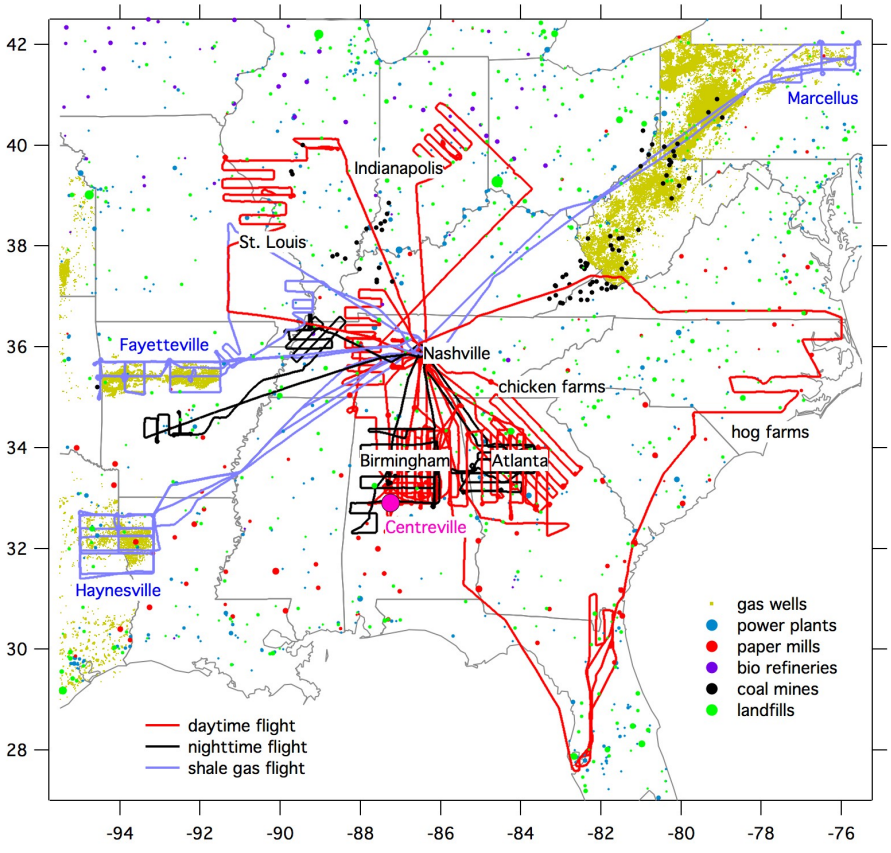

Figure 2: NOAA WP-3D flight tracks for daytime, nighttime and shale gas flights during SENEX. The marker size for the power plants is the annual gross load, for the paper mills the capacity, for the bio refineries the biofuel production, for the coal mines the methane emissions, and for the land fills the methane emissions.

Atmos. Meas. Tech. Discuss., doi:10.5194/amt-2015-388, 2016
Manuscript under review for journal Atmos. Meas. Tech.
Published: 20 January 2016

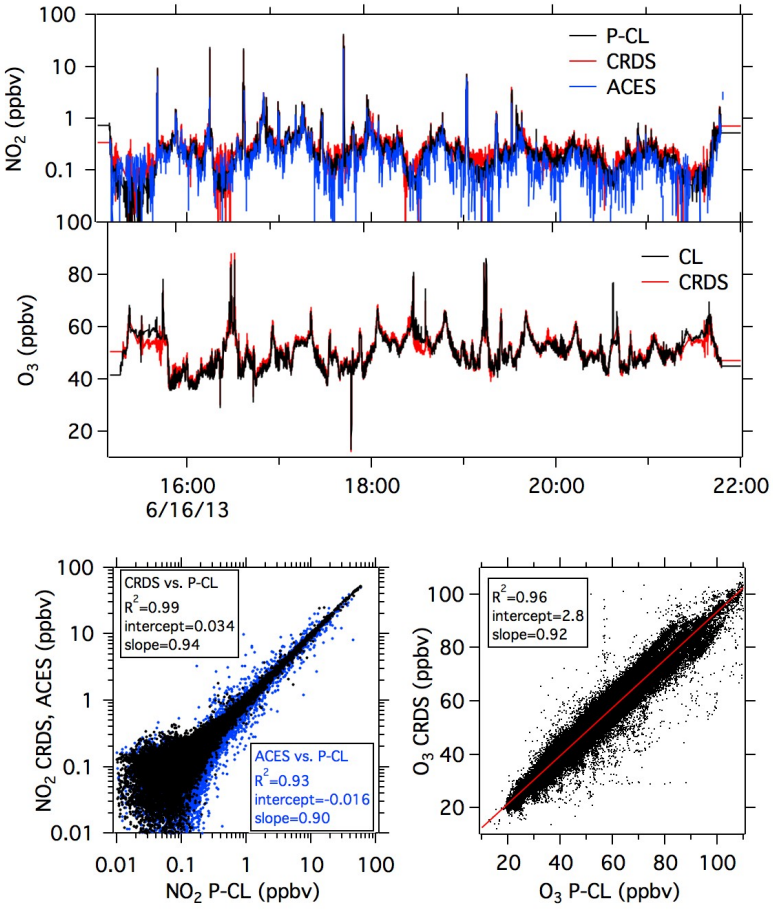

Figure 3: NO_2 inter-comparison between P-CL, CRDS and ACES instruments and ozone inter-comparison between P-CL and CRDS.

Atmos. Meas. Tech. Discuss., doi:10.5194/amt-2015-388, 2016
Manuscript under review for journal Atmos. Meas. Tech.
Published: 20 January 2016

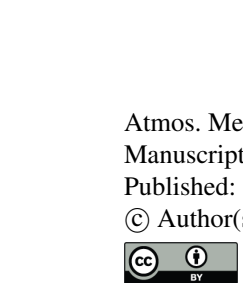

Atmospheric Measurement Techniques Discussions

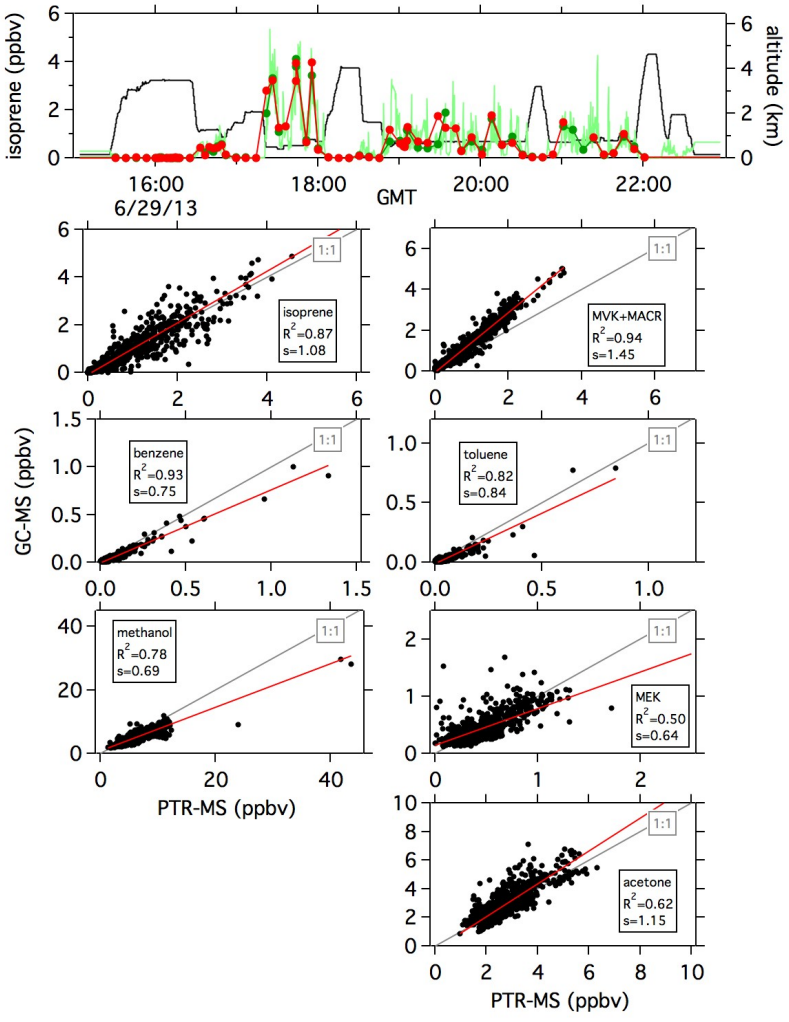

Figure 4: Inter-comparison between PTR-MS and iWAS/GCMS.

Atmos. Meas. Tech. Discuss., doi:10.5194/amt-2015-388, 2016
Manuscript under review for journal Atmos. Meas. Tech.
Published: 20 January 2016

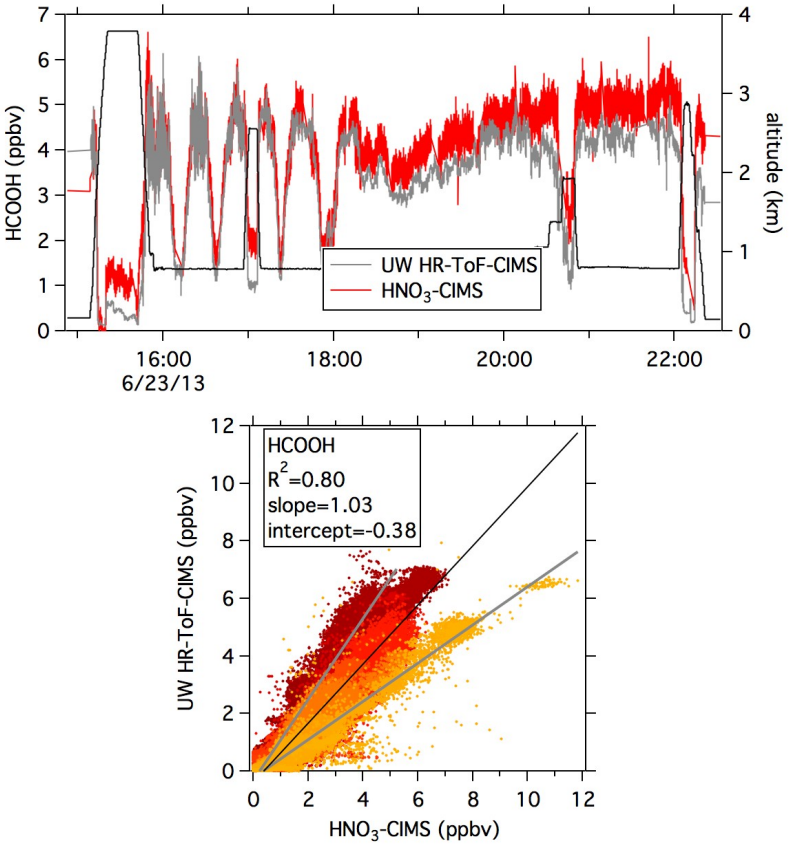

Figure 5: HCOOH inter-comparison between the HNO_3-CIMS and the UW HR-ToF-CIMS as a time series for a selected flight and a scatter plot. The color code in the scatter plot indicates all the individual flights. The black line is a fit using all the data the grey lines fits for individual flights with the highest or lowest slope, respectively.

Atmos. Meas. Tech. Discuss., doi:10.5194/amt-2015-388, 2016
Manuscript under review for journal Atmos. Meas. Tech.
Published: 20 January 2016

Atmospheric Measurement Techniques Discussions

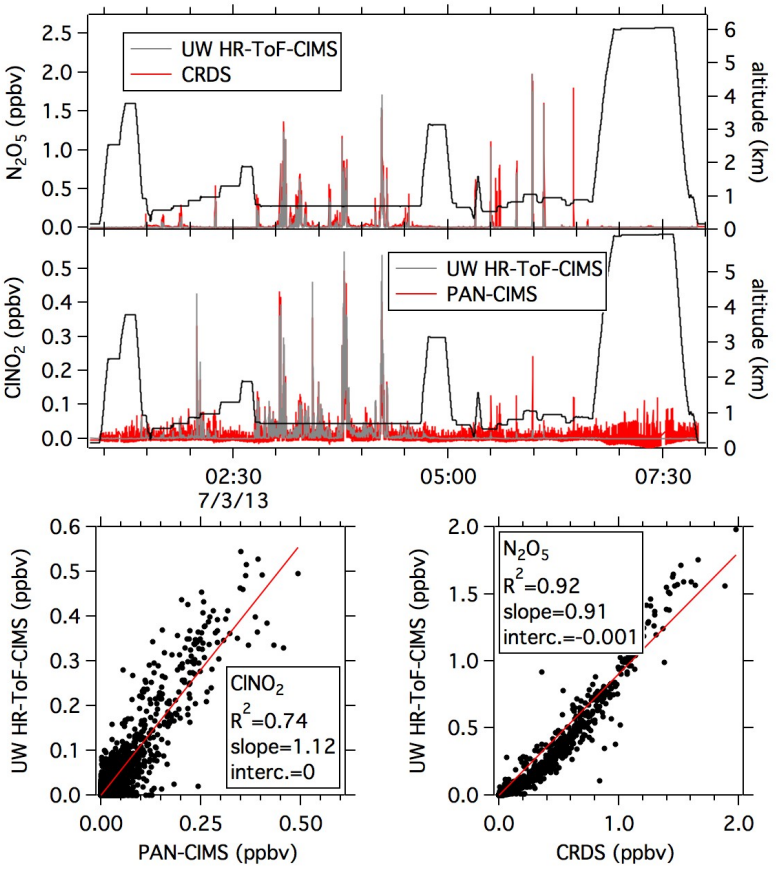

Figure 6: Inter-comparison between the UW HR-ToF-CIMS of N_2O_5 with CRDS and $ClNO_2$ with the PAN-CIMS as time series and scatter plots for the nighttime flight on 3 July 2013.

Atmos. Meas. Tech. Discuss., doi:10.5194/amt-2015-388, 2016
Manuscript under review for journal Atmos. Meas. Tech.
Published: 20 January 2016

Atmospheric Measurement Techniques Discussions

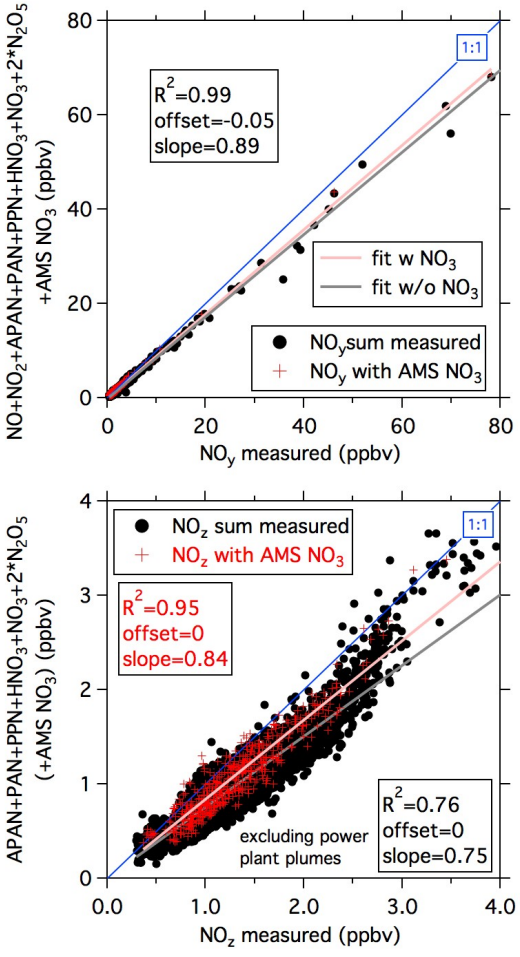

Figure 7: NO_y and NO_z (=NO_y-NO_x) budgets for the NOAA WP-3D flight on 16 June 2013 with and without aerosol nitrate.

Atmos. Meas. Tech. Discuss., doi:10.5194/amt-2015-388, 2016
Manuscript under review for journal Atmos. Meas. Tech.
Published: 20 January 2016

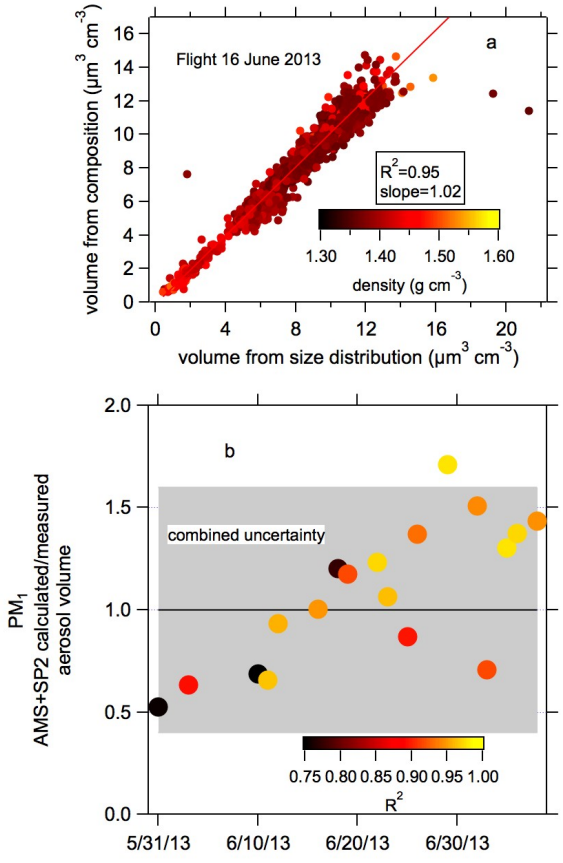

Figure 8: The aerosol volume derived from the chemical composition data (AMS and SP2) was compared to the volume from the size distribution data (NMASS and UHSAS). (a) The correlation for the flight on 16 June 2013 color-coded by the density. (b) The slopes for all the flights color-coded by the respective correlation coefficient determined as shown in (a).

Atmos. Meas. Tech. Discuss., doi:10.5194/amt-2015-388, 2016
Manuscript under review for journal Atmos. Meas. Tech.
Published: 20 January 2016

Atmospheric Measurement Techniques Discussions

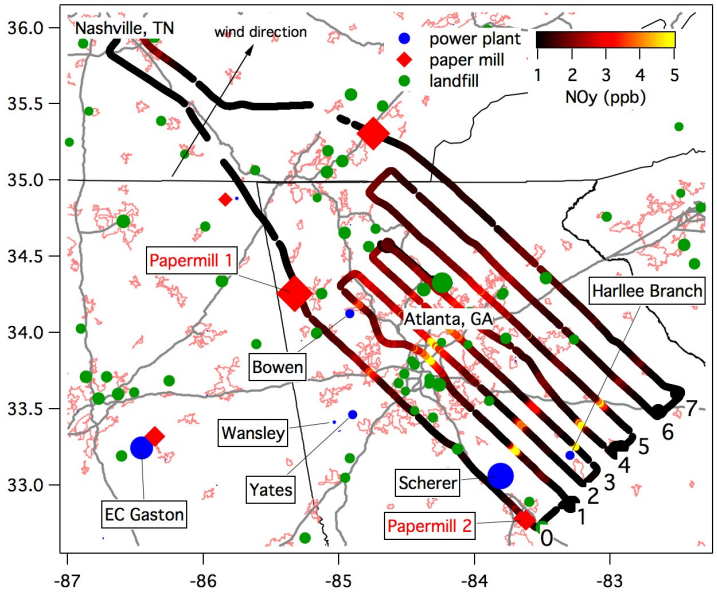

520

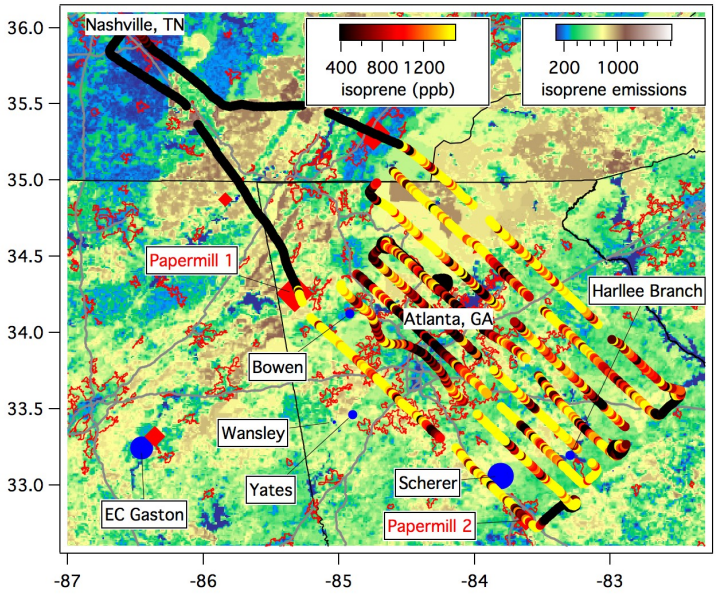

521
522
523 **Figure 9:** The flight track of the NOAA WP-3D on June 16, 2013 over Atlanta, GA color
524 coded with NO_y in the top panel and with isoprene on the bottom panel. The underlying
525 maps show the point source emissions (power plants, paper mills and land fills) in the top
526 panel and the isoprene emissions potential in the bottom panel.
527

Atmos. Meas. Tech. Discuss., doi:10.5194/amt-2015-388, 2016
Manuscript under review for journal Atmos. Meas. Tech.
Published: 20 January 2016

Atmospheric Measurement Techniques Discussions

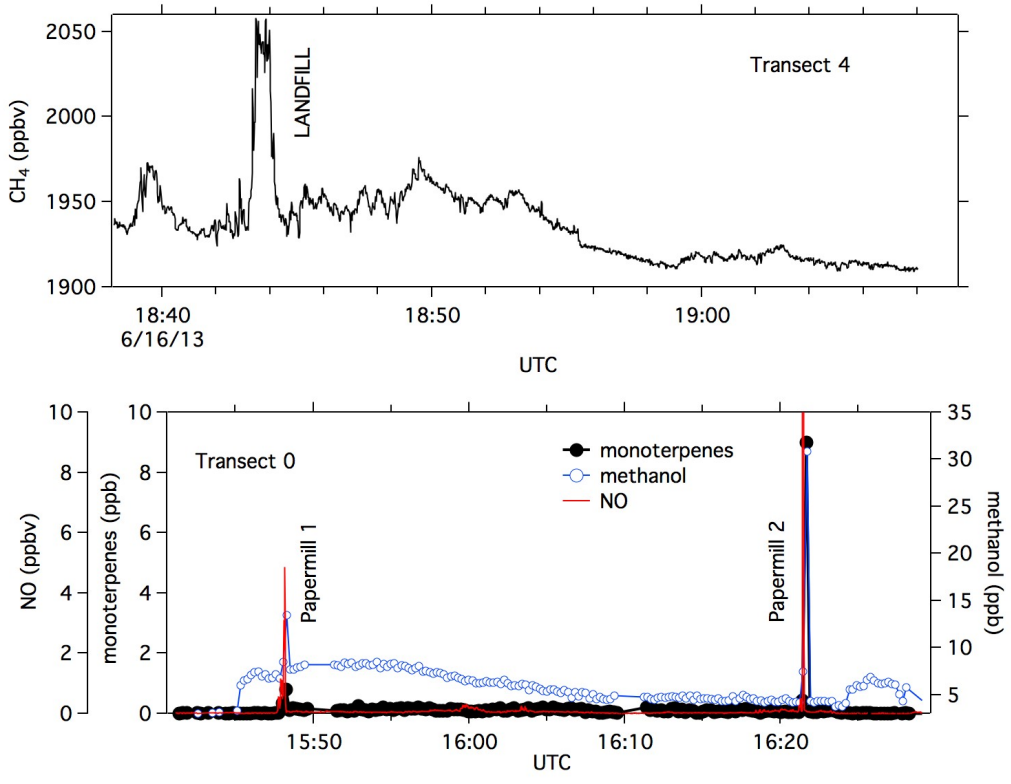

528
529
530 **Figure 10:** Time series of two transects during the 16 June 2013 flight downwind of a
531 landfill and two paper mills.
532
533

Atmos. Meas. Tech. Discuss., doi:10.5194/amt-2015-388, 2016
Manuscript under review for journal Atmos. Meas. Tech.
Published: 20 January 2016

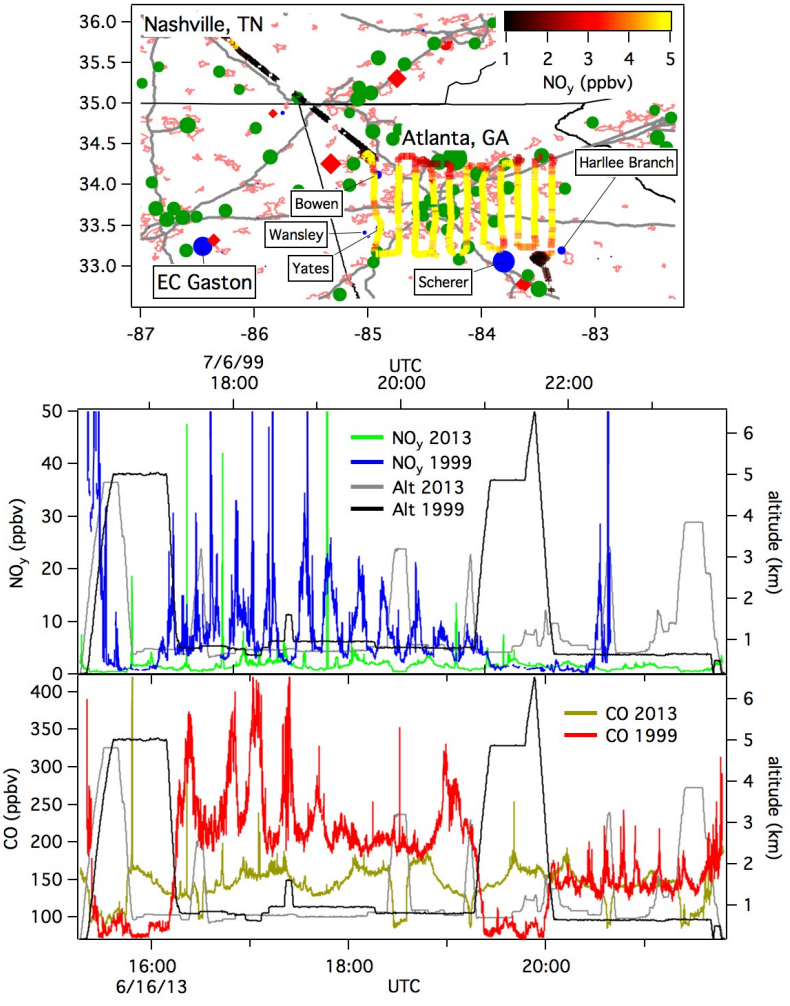

Figure 11: The track of a flight on 6 July 1999 over Atlanta during the SOS99 campaign color-coded with the NO_y mixing ratio. Time series of the 16 June 2013 and the 6 July 1999 flights for NO_y and CO show that the mixing ratios over Atlanta have decreased significantly over the past 14 years.

Atmos. Meas. Tech. Discuss., doi:10.5194/amt-2015-388, 2016
Manuscript under review for journal Atmos. Meas. Tech.
Published: 20 January 2016

Atmospheric Measurement Techniques Discussions

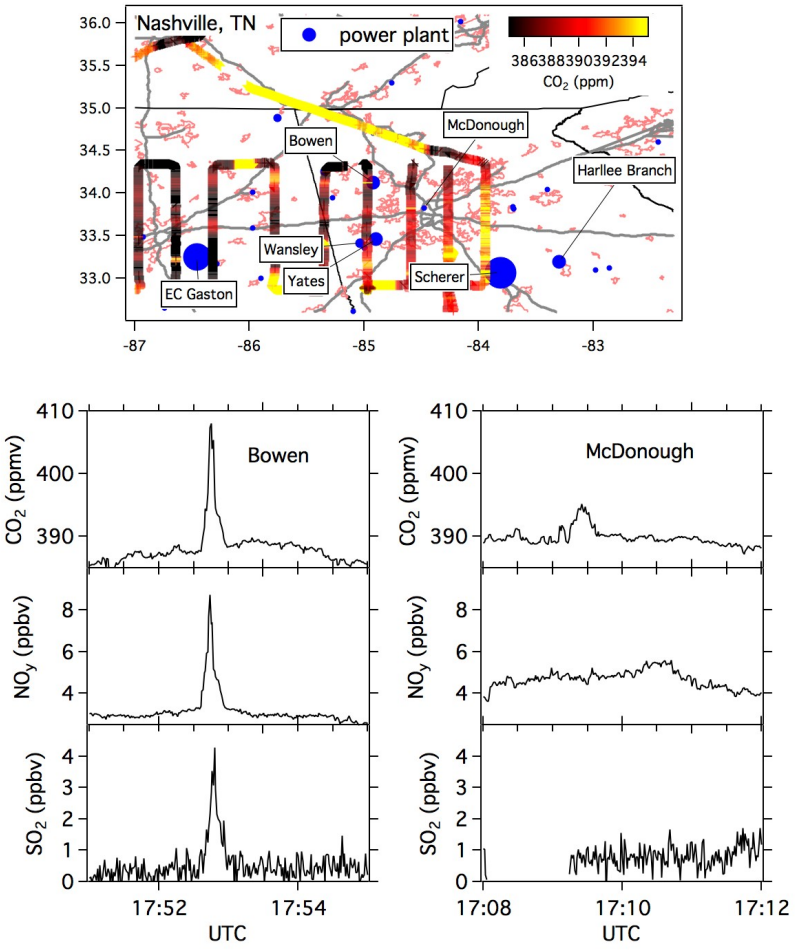

Figure 12: The track of a flight on 6 July 1999 over Atlanta during the SOS99 campaign color-coded with the NO_y mixing ratio. Time series of the 16 June 2013 and the 6 July 1999 flights for NO_y and CO show that the mixing ratios over Atlanta have decreased significantly over the past 14 years.

Atmos. Meas. Tech. Discuss., doi:10.5194/amt-2015-388, 2016
Manuscript under review for journal Atmos. Meas. Tech.
Published: 20 January 2016

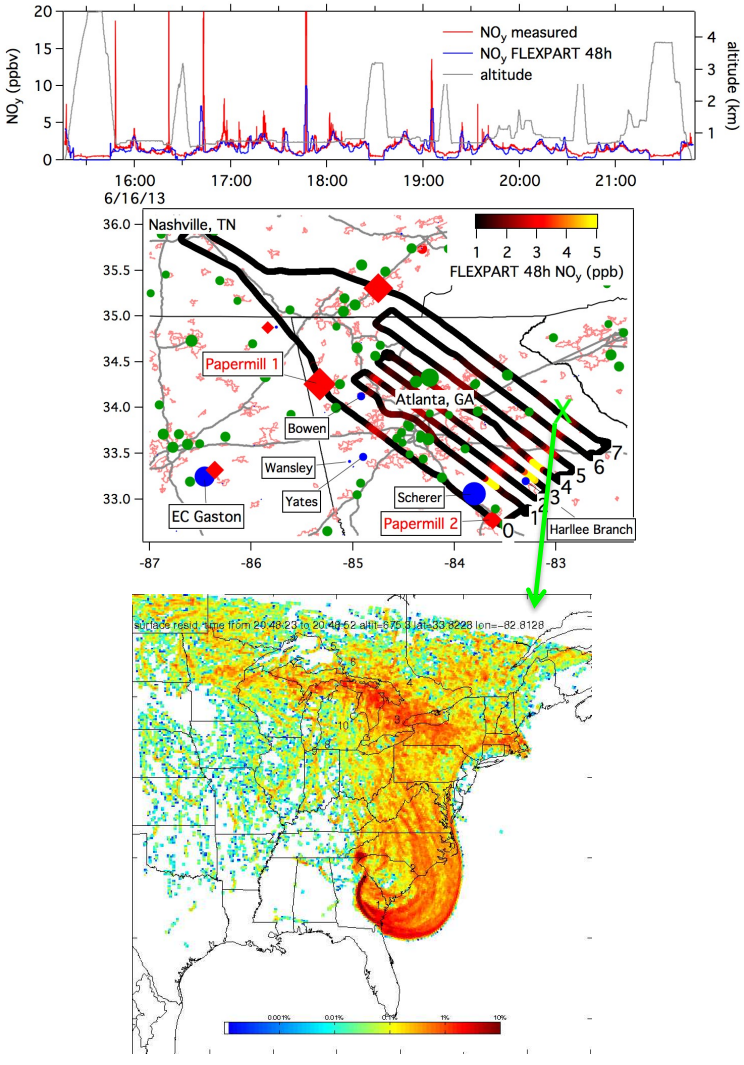

Figure 13: FLEXPART model results: time series of NO_y with 48 hours of accumulation time, the flight track color-coded by modeled NO_y and the surface residence time for a point on the last transect downwind of the Harllee Branch power plant.

Atmos. Meas. Tech. Discuss., doi:10.5194/amt-2015-388, 2016
Manuscript under review for journal Atmos. Meas. Tech.
Published: 20 January 2016

Atmospheric Measurement Techniques Discussions

559 **References:**
560
561 Bahreini, R., Dunlea, E. J., Matthew, B. M., Simons, C., Docherty, K. S., DeCarlo, P. F.,
562 Jimenez, J. L., Brock, C. A., and Middlebrook, A. M.: Design and operation of a pressure-
563 controlled inlet for airborne sampling with an aerodynamic aerosol lens, Aerosol Sci.
564 Technol., 42, 465-471, 2008.

565 Bahreini, R., Ervens, B., Middlebrook, A. M., Warneke, C., de Gouw, J. A., DeCarlo, P. F.,
566 Jimenez, J. L., Brock, C. A., Neuman, J. A., Ryerson, T. B., Stark, H., Atlas, E., Brioude, J., Fried,
567 A., Holloway, J. S., Peischl, J., Richter, D., Walega, J., Weibring, P., Wollny, A. G., and
568 Fehsenfeld, F. C.: Organic aerosol formation in urban and industrial plumes near Houston
569 and Dallas, Texas, J. Geophys. Res.-Atmos., 114, 2009.

570 Brock, C. A., Cozic, J., Bahreini, R., Froyd, K. D., Middlebrook, A. M., McComiskey, A.,
571 Brioude, J., Cooper, O. R., Stohl, A., Aikin, K. C., de Gouw, J. A., Fahey, D. W., Ferrare, R. A.,
572 Gao, R. S., Gore, W., Holloway, J. S., Hubler, G., Jefferson, A., Lack, D. A., Lance, S., Moore, R.
573 H., Murphy, D. M., Nenes, A., Novelli, P. C., Nowak, J. B., Ogren, J. A., Peischl, J., Pierce, R. B.,
574 Pilewskie, P., Quinn, P. K., Ryerson, T. B., Schmidt, K. S., Schwarz, J. P., Sodemann, H.,
575 Spackman, J. R., Stark, H., Thomson, D. S., Thornberry, T., Veres, P., Watts, L. A., Warneke, C.,
576 and Wollny, A. G.: Characteristics, sources, and transport of aerosols measured in spring
577 2008 during the aerosol, radiation, and cloud processes affecting Arctic Climate (ARCPAC)
578 Project, Atmos. Chem. Phys., 11, 2423-2453, 2011.

579 Brock, C. A., Schroder, F., Bernd, K., Petzold, A., Busen, R., and Fiebig, M.: Ultrafine
580 particle size distributions measured in aircraft exhaust plumes, J. Geophys. Res., 105,
581 26,555-526,567, 2000.

582 Cazorla, M., Wolfe, G. M., Bailey, S. A., Swanson, A. K., Arkinson, H. L., and Hanisco, T.
583 F.: A new airborne laser-induced fluorescence instrument for in situ detection of
584 formaldehyde throughout the troposphere and lower stratosphere, Atmospheric
585 Measurement Techniques, 8, 541-552, 2015.

586 Chang, W. L., Bhave, P. V., Brown, S. S., Riemer, N., Stutz, J., and Dabdub, D.:
587 Heterogeneous Atmospheric Chemistry, Ambient Measurements, and Model Calculations
588 of N2O5: A Review, Aerosol Science and Technology, 45, 665-695, 2011.

589 Cross, E. S., Slowik, J. G., Davidovits, P., Allan, J. D., Worsnop, D. R., Jayne, J. T., Lewis,
590 D. K., Canagaratna, M., and Onasch, T. B.: Laboratory and ambient particle density
591 determinations using light scattering in conjunction with aerosol mass spectrometry,
592 Aerosol Sci. Technol., 41, 343-359, 2007.

593 Dallmann, T. R. and Harley, R. A.: Evaluation of mobile source emission trends in
594 the United States, J. Geophys. Res.-Atmos., 115, 2010.

595 de Gouw, J. A., McKeen, S. A., Aikin, K. C., Brock, C. A., Brown, S. S., Gilman, J. B., Graus,
596 M., Hanisco, T., Holloway, J. S., Kaiser, J., Keutsch, F. N., Lerner, B. M., Liao, J., Markovic, M. Z.,
597 Middlebrook, A. M., Min, K. E., Neuman, J. A., Nowak, J. B., Peischl, J., Pollack, I. B., Roberts, J.

598 M., Ryerson, T. B., Trainer, M., Veres, P. R., Warneke, C., Welti, A., and Wolfe, G. M.: Airborne
599 measurements of the atmospheric emissions from a fuel ethanol refinery, J. Geophys. Res.-
600 Atmos., 120, 4385-4397, 2015a.

601 de Gouw, J. A., Parrish, D. D., Frost, G. J., and Trainer, M.: Reduced emissions of CO2,
602 NOx, and SO2 from US power plants owing to switch from coal to natural gas with
603 combined cycle technology, Earths Future, 2, 75-82, 2014.

604 de Gouw, J. A., Trainer, M., Brown, S. S., Edwards, P., Gilman, J. B., Graus, M., Hanisco,
605 T., Kaiser, J., Keutsch, F. N., Kim, S. W., Lerner, B. M., Neuman, J. A., Parrish, D. D., Pollack, I.
606 B., Roberts, J. M., Ryerson, T. R., Veres, P. R., Warneke, C., and Wolfe, G. M.: Enhanced
607 Removal of Biogenic Hydrocarbons in Power Plant Plumes Constrains the Dependence of
608 Atmospheric Hydroxyl Concentrations on Nitrogen Oxides, Geophys. Res. Lett., in
609 preparation, 2015b.

610 de Gouw, J. A. and Warneke, C.: Measurements of volatile organic compounds in the
611 earths atmosphere using proton-transfer-reaction mass spectrometry, Mass Spectrometry
612 Reviews, 26, 223-257, 2007.

613 DiGangi, J. P., Boyle, E. S., Karl, T., Harley, P., Turnipseed, A., Kim, S., Cantrell, C.,
614 Maudlin, R. L., III, Zheng, W., Flocke, F., Hall, S. R., Ullmann, K., Nakashima, Y., Paul, J. B.,
615 Wolfe, G. M., Desai, A. R., Kajii, Y., Guenther, A., and Keutsch, F. N.: First direct
616 measurements of formaldehyde flux via eddy covariance: implications for missing in-
617 canopy formaldehyde sources, Atmos. Chem. Phys., 11, 10565-10578, 2011.

618 Dube, W. P., Brown, S. S., Osthoff, H. D., Nunley, M. R., Ciciora, S. J., Paris, M. W.,
619 McLaughlin, R. J., and Ravishankara, A. R.: Aircraft instrument for simultaneous, in situ
620 measurement of NO3 and N2O5 via pulsed cavity ring-down spectroscopy, Rev. Sci. Instr.,
621 77, 2006.

622 Emmons, L. K., Arnold, S. R., Monks, S. A., Huijnen, V., Tilmes, S., Law, K. S., Thomas, J.
623 L., Raut, J. C., Bouarar, I., Turquety, S., Long, Y., Duncan, B., Steenrod, S., Strode, S.,
624 Flemming, J., Mao, J., Langner, J., Thompson, A. M., Tarasick, D., Apel, E. C., Blake, D. R.,
625 Cohen, R. C., Dibb, J., Diskin, G. S., Fried, A., Hall, S. R., Huey, L. G., Weinheimer, A. J.,
626 Wisthaler, A., Mikoviny, T., Nowak, J., Peischl, J., Roberts, J. M., Ryerson, T., Warneke, C., and
627 Helmig, D.: The POLARCAT Model Intercomparison Project (POLMIP): overview and
628 evaluation with observations, Atmos. Chem. Phys., 15, 6721-6744, 2015.

629 Gilman, J. B., Kuster, W. C., Goldan, P. D., Herndon, S. C., Zahniser, M. S., Tucker, S. C.,
630 Brewer, W. A., Lerner, B. M., Williams, E. J., Harley, R. A., Fehsenfeld, F. C., Warneke, C., and
631 de Gouw, J. A.: Measurements of volatile organic compounds during the 2006
632 TexAQS/GoMACCS campaign: Industrial influences, regional characteristics, and diurnal
633 dependencies of the OH reactivity, J. Geophys. Res.-Atmos., 114, 2009.

634 Holloway, J. S., Jakoubek, R. O., Parrish, D. D., Gerbig, C., Volz-Thomas, A., Schmitgen,
635 S., Fried, A., Wert, B., Henry, B., and Drummond, J. R.: Airborne intercomparison of vacuum

636 ultraviolet fluorescence and tunable diode laser absorption measurements of tropospheric
637 carbon monoxide, J. Geophys. Res., 105, 24,251-224,261, 2000.

638 Hottle, J. R., Huisman, A. J., Digangi, J. P., Kammrath, A., Galloway, M. M., Coens, K. L.,
639 and Keutsch, F. N.: A Laser Induced Fluorescence-Based Instrument for In-Situ
640 Measurements of Atmospheric Formaldehyde, Environ. Sci. Technol., 43, 790-795, 2009.

641 Kaiser, J., Wolfe, G. M., Min, K. E., Brown, S. S., Miller, C. C., Jacob, D. J., deGouw, J. A.,
642 Graus, M., Hanisco, T. F., Holloway, J., Peischl, J., Pollack, I. B., Ryerson, T. B., Warneke, C.,
643 Washenfelder, R. A., and Keutsch, F. N.: Reassessing the ratio of glyoxal to formaldehyde as
644 an indicator of hydrocarbon precursor speciation, Atmos. Chem. Phys., 15, 7571-7583,
645 2015.

646 Kercher, J. P., Riedel, T. P., and Thornton, J. A.: Chlorine activation by N2O5:
647 simultaneous, in situ detection of ClNO2 and N2O5 by chemical ionization mass
648 spectrometry, Atmospheric Measurement Techniques, 2, 193-204, 2009.

649 Kiendler-Scharr, A., Zhang, Q., Hohaus, T., Kleist, E., Mensah, A., Mentel, T. F.,
650 Spindler, C., Uerlings, R., Tillmann, R., and Wildt, J.: Aerosol mass spectrometric features of
651 biogenic SOA: Observations from a plant chamber and in rural atmospheric environments,
652 Environ. Sci. Technol., 43, 8166-8172, 2009.

653 Lack, D. A., Richardson, M. S., Law, D., Langridge, J. M., Cappa, C. D., McLaughlin, R. J.,
654 and Murphy, D. M.: Aircraft Instrument for Comprehensive Characterization of Aerosol
655 Optical Properties, Part 2: Black and Brown Carbon Absorption and Absorption
656 Enhancement Measured with Photo Acoustic Spectroscopy, Aerosol Science and
657 Technology, 46, 555-568, 2012.

658 Lance, S., Brock, C. A., Rogers, D., and Gordon, J. A.: Water droplet calibration of the
659 Cloud Droplet Probe (CDP) and in-flight performance in liquid, ice and mixed-phase clouds
660 during ARCPAC, Atmospheric Measurement Techniques, 3, 1683-1706, 2010.

661 Lance, S., Medina, J., Smith, J. N., and Nenes, A.: Mapping the operation of the DMT
662 Continuous Flow CCN counter, Aerosol Science and Technology, 40, 242-254, 2006.

663 Langridge, J. M., Richardson, M. S., Lack, D., Law, D., and Murphy, D. M.: Aircraft
664 Instrument for Comprehensive Characterization of Aerosol Optical Properties, Part I:
665 Wavelength-Dependent Optical Extinction and Its Relative Humidity Dependence
666 Measured Using Cavity Ringdown Spectroscopy, Aerosol Science and Technology, 45,
667 1305-1318, 2011.

668 Lee, B. H., Lopez-Hilfiker, F. D., Mohr, C., Kurten, T., Worsnop, D. R., and Thornton, J.
669 A.: An Iodide-Adduct High-Resolution Time-of-Flight Chemical-Ionization Mass
670 Spectrometer: Application to Atmospheric Inorganic and Organic Compounds, Environ. Sci.
671 Technol., 48, 6309-6317, 2014.

672 Lerner, B., Gilman, J. B., Dumas, M., Hughes, D. D., Jaksich, A., Hatch, C. D., Graus, M.,
673 Tokarek, T. W., Peischl, J., Koss, A., Yuan, B., Warneke, C., Isaacman-Van Wertz, G., Sueper,
674 D., and de Gouw, J. A.: An improved, automated whole-air sampler and VOC GC-MS analysis
675 system, Atmospheric measurement Techniques Discussions, in preparation, 2015.

676 Middlebrook, A. M., Bahreini, R., Jimenez, J. L., and Canagaratna, M. R.: Evaluation of
677 composition-dependent collection efficiencies for the Aerodyne aerosol mass
678 spectrometer using field data, Aerosol Sci. Technol., 46, 258-271, 2012.

679 Min, K. E., Washenfelder, R. A., Dube, W. P., Langford, A. O., Edwards, P. M., Zarzana,
680 K. J., Stutz, J., Lu, K., Zhang, Y., and Brown, S. S.: A broadband cavity enhanced absorption
681 spectrometer for aircraft measurements of glyoxal, methyl glyoxal, nitrous acid, nitrogen
682 dioxide, and water vapor, Atmospheric measurement Techniques Discussions, submitted,
683 2015.

684 Neuman, J. A., Huey, L. G., Dissly, R. W., Fehsenfeld, F. C., Flocke, F., Holecek, J. C.,
685 Holloway, J. S., Hubler, G., Jakoubek, R., Nicks Jr., D. K., Parrish, D. D., Ryerson, T. B., Sueper,
686 D. T., and Weinheimer, A. J.: Fast-response airborne in situ measurements of HNO3 during
687 the Texas 2000 Air Quality Study, J. Geophys. Res., 107, 4436,
688 doi:4410.1029/2001JD001437, 2002.

689 Neuman, J. A., Ryerson, T. B., Huey, L. G., Jakoubek, R., Nowak, J. B., Simons, C., and
690 Fehsenfeld, F. C.: Calibration and evaluation of nitric acid and ammonia permeation tubes
691 by UV optical absorption, Environ. Sci. Technol., 37, 2975-2981, 2003.

692 Nowak, J. B., Neuman, J. A., Kozai, K., Huey, L. G., Tanner, D. J., Holloway, J. S.,
693 Ryerson, T. B., Frost, G. J., McKeen, S. A., and Fehsenfeld, F. C.: A chemical ionization mass
694 spectrometry technique for airborne measurements of ammonia, J. Geophys. Res.-Atmos.,
695 112, 2007.

696 Osthoff, H. D., Roberts, J. M., Ravishankara, A. R., Williams, E. J., Lerner, B. M.,
697 Sommariva, R., Bates, T. S., Coffman, D., Quinn, P. K., Dibb, J. E., Stark, H., Burkholder, J. B.,
698 Talukdar, R. K., Meagher, J., Fehsenfeld, F. C., and Brown, S. S.: High levels of nitryl chloride
699 in the polluted subtropical marine boundary layer, Nature Geoscience, 1, 324-328, 2008.

700 Park, K., Kittelson, D. B., Zachariah, M. R., and McMurry, P. H.: Measurement of
701 inherent material density of nanoparticle agglomerates, J. Nanoparticle Res., 6, 267-272,
702 2004.

703 Peischl, J., Ryerson, T. B., Aikin, K. C., de Gouw, J. A., Gilman, J. B., Holloway, J. S.,
704 Lerner, B. M., Nadkarni, R., Neuman, J. A., Nowak, J. B., Trainer, M., Warneke, C., and Parrish,
705 D. D.: Quantifying atmospheric methane emissions from the Haynesville, Fayetteville, and
706 northeastern Marcellus shale gas production regions, J. Geophys. Res.-Atmos., 120, 2119-
707 2139, 2015.

708 Peischl, J., Ryerson, T. B., Holloway, J. S., Trainer, M., Andrews, A. E., Atlas, E. L.,
709 Blake, D. R., Daube, B. C., Dlugokencky, E. J., Fischer, M. L., Goldstein, A. H., Guha, A., Karl, T.,

710 Kofler, J., Kosciuch, E., Misztal, P. K., Perring, A. E., Pollack, I. B., Santoni, G. W., Schwarz, J. P.,
711 Spackman, J. R., Wofsy, S. C., and Parrish, D. D.: Airborne observations of methane
712 emissions from rice cultivation in the Sacramento Valley of California, J. Geophys. Res.-
713 Atmos., 117, 2012.

714 Perry, R. H. and Green, D. W. (Eds.): Perry's Chemical Engineers' Handbook,
715 McGraw-Hill, New York, NY, 1997.

716 Pollack, I. B., Lerner, B. M., and Ryerson, T. B.: Evaluation of ultraviolet light-
717 emitting diodes for detection of atmospheric NO2 by photolysis - chemiluminescence,
718 Journal of Atmospheric Chemistry, 65, 111-125, 2010.

719 Roberts, G. C. and Nenes, A.: A continuous-flow streamwise thermal-gradient CCN
720 chamber for atmospheric measurements, Aerosol Science and Technology, 39, 206-221,
721 2005.

722 Ryerson, T. B., Buhr, M. P., Frost, G. J., Goldan, P. D., Holloway, J. S., Hübler, G., Jobson,
723 B. T., Kuster, W. C., McKeen, S. A., Parrish, D. D., Roberts, J. M., Sueper, D. T., Trainer, M.,
724 Williams, J., and Fehsenfeld, F. C.: Emissions lifetimes and ozone formation in power plant
725 plumes, J. Geophys. Res., 103, 22,569-522,583, 1998.

726 Ryerson, T. B., Huey, L. G., Knapp, K., Neuman, J. A., Parrish, D. D., Sueper, D. T., and
727 Fehsenfeld, F. C.: Design and initial characterization of an inlet for gas-phase NO_y
728 measurements from aircraft, J. Geophys. Res., 104, 5483-5492, 1999.

729 Schwarz, J. P., Gao, R. S., Fahey, D. W., Thomson, D. S., Watts, L. A., Wilson, J. C.,
730 Reeves, J. M., Darbeheshti, M., Baumgardner, D. G., Kok, G. L., Chung, S. H., Schulz, M.,
731 Hendricks, J., Lauer, A., Kaercher, B., Slowik, J. G., Rosenlof, K. H., Thompson, T. L., Langford,
732 A. O., Loewenstein, M., and Aikin, K. C.: Single-particle measurements of midlatitude black
733 carbon and light-scattering aerosols from the boundary layer to the lower stratosphere, J.
734 Geophys. Res.-Atmos., 111, D16207, 2006.

735 Schwarz, J. P., Spackman, J. R., Fahey, D. W., Gao, R. S., Lohmann, U., Stier, P., Watts, L.
736 A., Thomson, D. S., Lack, D. A., Pfister, L., Mahoney, M. J., Baumgardner, D., Wilson, J. C., and
737 Reeves, J. M.: Coatings and their enhancement of black carbon light absorption in the
738 tropical atmosphere, J. Geophys. Res.-Atmos., 113, 2008.

739 Schwarz, J. P., Spackman, J. R., Gao, R. S., Watts, L. A., Stier, P., Schulz, M., Davis, S. M.,
740 Wofsy, S. C., and Fahey, D. W.: Global-scale black carbon profiles observed in the remote
741 atmosphere and compared to models (vol 37, art L18812 , 2010), Geophys. Res. Lett., 37,
742 2010.

743 Slusher, D. L., Huey, L. G., Tanner, D. J., Flocke, F. M., and Roberts, J. M.: A thermal
744 dissociation-chemical ionization mass spectrometry (TD-CIMS) technique for the
745 simultaneous measurement of peroxyacyl nitrates and dinitrogen pentoxide, J. Geophys.
746 Res.-Atmos., 109, 2004.

747 Stohl, A., Forster, C., Frank, A., Seibert, P., and Wotawa, G.: Technical Note : The
748 Lagrangian particle dispersion model FLEXPART version 6.2, Atmos. Chem. Phys., 5, 2461-
749 2474, 2005.

750 Veres, P., Gilman, J. B., Roberts, J. M., Kuster, W. C., Warneke, C., Burling, I. R., and de
751 Gouw, J.: Development and validation of a portable gas phase standard generation and
752 calibration system for volatile organic compounds, Atmospheric Measurement Techniques,
753 3, 683-691, 2010.

754 von Schneidemesser, E., Monks, P. S., and Plass-Duelmer, C.: Global comparison of
755 VOC and CO observations in urban areas, Atmos. Environ., 44, 5053-5064, 2010.

756 Wagner, N. L., Dube, W. P., Washenfelder, R. A., Young, C. J., Pollack, I. B., Ryerson, T.
757 B., and Brown, S. S.: Diode laser-based cavity ring-down instrument for NO3, N2O5, NO,
758 NO2 and O-3 from aircraft, Atmospheric Measurement Techniques, 4, 1227-1240, 2011.

759 Warneke, C., de Gouw, J. A., Holloway, J. S., Peischl, J., Ryerson, T. B., Atlas, E., Blake,
760 D., Trainer, M., and Parrish, D. D.: Multiyear trends in volatile organic compounds in Los
761 Angeles, California: Five decades of decreasing emissions, J. Geophys. Res.-Atmos., 117,
762 2012.

763 Warneke, C., Roberts, J. M., Veres, P., Gilman, J., Kuster, W. C., Burling, I., Yokelson, R.,
764 and de Gouw, J. A.: VOC identification and inter-comparison from laboratory biomass
765 burning using PTR-MS and PIT-MS, International Journal of Mass Spectrometry, 303, 6-14,
766 2011.

767 Washenfelder, R. A., Young, C. J., Brown, S. S., Angevine, W. M., Atlas, E. L., Blake, D.
768 R., Bon, D. M., Cubison, M. J., de Gouw, J. A., Dusanter, S., Flynn, J., Gilman, J. B., Graus, M.,
769 Griffith, S., Grossberg, N., Hayes, P. L., Jimenez, J. L., Kuster, W. C., Lefer, B. L., Pollack, I. B.,
770 Ryerson, T. B., Stark, H., Stevens, P. S., and Trainer, M. K.: The glyoxal budget and its
771 contribution to organic aerosol for Los Angeles, California, during CalNex 2010, J. Geophys.
772 Res.-Atmos., 116, 2011.

773 Wilson, J. C., Lafleur, B. G., Hilbert, H., Seebaugh, W. R., Fox, J., Gesler, D. W., Brock, C.
774 A., Huebert, B. J., and Mullen, J.: Function and performance of a low turbulence inlet for
775 sampling supermicron particles from aircraft platforms, Aerosol Science and Technology,
776 38, 790-802, 2004.

777 Wolfe, G. M., Kaiser, J., Hanisco, T. F., Keutsch, F. N., de Gouw, J. A., Gilman, J. B.,
778 Graus, M., Hatch, C. D., Holloway, J., Horowitz, L., Lee, B. H., Lerner, B., Lopez-Hilfiker, F. D.,
779 Mao, J., Marvin, M., Peischl, J., Pollack, I. B., Roberts, J. M., Ryerson, T. B., Thornton, J. A.,
780 Veres, P., and Warneke, C.: Formaldehyde production from isoprene oxidation across NOx
781 regimes, in preparation, 2015. 2015.

782 Xu, L., Guo, H., Boyd, C. M., Klein, M., Bougiatioti, A., Cerully, K. M., Hite, J. R.,
783 Isaacman-VanWertz, G., Kreisberg, N. M., Knote, C., Olson, K., Koss, A., Goldstein, A. H.,
784 Hering, S. V., de Gouw, J., Baumann, K., Lee, S.-H., Nenes, A., Weber, R. J., and Ng, N. L.:

785 Effects of anthropogenic emissions on aerosol formation from isoprene and monoterpenes
786 in the southeastern United States, Proceedings of the National Academy of Sciences of the
787 United States of America, 112, 37-42, 2015.

788 Yu, H.: Development of landcover and emission factors for isoprene and
789 monoterpene emission modeling and evaluation in the southern United States using
790 airborne direct and indirect flux measurements, 2015. 2015.

791 Yuan, B., Kaser, L., Karl, T., Graus, M., Peischl, J., Campos, T. L., Shertz, S., Apel, E. C.,
792 Hornbrook, R. S., Hills, A., Gilman, J. B., Lerner, B. M., Warneke, C., Flocke, F. M., Ryerson, T.
793 B., Guenther, A. B., and de Gouw, J. A.: Airborne flux measurements of methane and volatile
794 organic compounds over the Haynesville and Marcellus shale gas production regions,
795 Journal of Geophysical Research: Atmospheres, 120, 6271-6289, 2015.

796 Zelenyuk, A., Imre, D., Han, J. H., and Oatis, S.: Simultaneous measurements of
797 individual ambient particle size, composition, effective density, and hygroscopicity, Anal.
798 Chem., 80, 1401-1407, 2008.

799 Zheng, W., Flocke, F. M., Tyndall, G. S., Swanson, A., Orlando, J. J., Roberts, J. M., Huey,
800 L. G., and Tanner, D. J.: Characterization of a thermal decomposition chemical ionization
801 mass spectrometer for the measurement of peroxy acyl nitrates (PANs) in the atmosphere,
802 Atmos. Chem. Phys., 11, 6529-6547, 2011.
803
804